Biomedicine & Pharmacotherapy 165 (2023) 115146

Contents lists available at ScienceDirect

Biomedicine & Pharmacotherapy

journal homepage: www.elsevier.com/locate/biopha

Novel bioprinted 3D model to human fibrosis investigation

Tiziana Petrachi [a], Alberto Portone [a], Gaëlle Françoise Arnaud [a,b,c,d], Francesco Ganzerli [a], Valentina Bergamini [a,b], Elisa Resca [a], Luca Accorsi [a], Alberto Ferrari [a,c], Annalisa Delnevo [a], Luigi Rovati [c], Caterina Marra [d], Chiara Chiavelli [d], Massimo Dominici [d,1,2], Elena Veronesi [a,*,1,2]

[a] Technopole "Mario Veronesi", via 29 Maggio 6, 41037 Mirandola, Italy
[b] Clinical and Experimental Medicine PhD program, University of Modena and Reggio Emilia, Italy
[c] Department of Engineering "Enzo Ferrari", University of Modena and Reggio Emilia, via Vivarelli, 10, Building 26, 41124 Modena, Italy
[d] Department of Medical and Surgical Sciences for Children & Adults, University of Modena and Reggio Emilia, Hospital of Modena, Via del Pozzo, 71, 44125 Modena, Italy

ARTICLE INFO

Keywords:
Fibrosis
Bioprinting
Disease modeling, testing, extracellular matrix

ABSTRACT

Fibrosis is shared in multiple diseases with progressive tissue stiffening, organ failure and limited therapeutic options. This unmet need is also due to the lack of adequate pre-clinical models to mimic fibrosis and to be challenged novel by anti-fibrotic therapeutic venues. Here using bioprinting, we designed a novel 3D model where normal human healthy fibroblasts have been encapsulated in type I collagen. After stimulation by Transforming Growth factor beta (TGFβ), embedded cells differentiated into myofibroblasts and enhanced the contractile activity, as confirmed by the high level of α − smooth muscle actin (αSMA) and F-actin expression. As functional assays, SEM analysis revealed that after TGFβ stimulus the 3D microarchitecture of the scaffold was dramatically remolded with an increased fibronectin deposition with an abnormal collagen fibrillar pattern. Picrius Sirius Red staining additionally revealed that TGFβ stimulation enhanced of two logarithm the collagen fibrils neoformation in comparison with control. These data indicate that by bioprinting technology, it is possible to generate a reproducible and functional 3D platform to mimic fibrosis as key tool for drug discovery and impacting on animal experimentation and reducing costs and time in addressing fibrosis.

1. Introduction

Fibrosis is a long-lasting pathological phenotype occurring in nearly every tissue and organ in the body as a final outcome of the abnormal tissue repair [1]. The condition is characterized by an exacerbated and repetitive accumulation of ECM proteins resulting in a severe alteration of tissue architecture and ultimately in an irreversible organ failure [2].

Although the complex mechanisms leading to tissue fibrosis are not yet fully understood, it has been amply demonstrated that pathological fibroplasia is originated by an early inflammatory phase in which immune cells start to release soluble factors able to activate fibroblasts for ECM remodeling.

One of the key regulators of ECM is the Transforming Growth Factor Beta (TGF β)[3–6]a peculiar cytokine responsible for the transactivation of fibroblast into contractile myofibroblasts overexpressing α-smooth muscle actin (αSMA) and secreting abnormal excessive ECM proteins [7]. For this reason, the most common tools used to study the fibrosis are two-dimensional (2D) cell culture models stimulated by exogenous profibrotic factor, such as TGFβ [8].

Although these are relatively simple and reproducible approaches they may lack of the predictivity [9,10]. For instance, these 2D systems are not able to recapitulate the complexity of a 3D spatial organization, cell-cell or cell-matrix interactions, mechanical forces as well as physiological oxygen, nutrient and signaling gradients [11–14]. Another limit of 2D cultures is the use of a plastic-based stiff substrate different from the one present during fibrosis. Balestrini et al. have demonstrated that tissue culture plasticware and stiff collagen coated silicon substrate can alter fibroblast proliferation rate and αSMA expression if compared with cells expanded on softer substrate [15].

On the other hand, authors report genetically modified or fibrosis-

* Corresponding author.
E-mail address: elena.veronesi@tpm.bio (E. Veronesi).
[1] These authors equally contributed to the manuscript
[2] Elena Veronesi and Massimo Dominici are co-last authors.

https://doi.org/10.1016/j.biopha.2023.115146
Received 28 February 2023; Received in revised form 5 July 2023; Accepted 7 July 2023
Available online 17 July 2023

induced animal models to improve an in vivo knowledge of molecular feature in fibrosis [16]. While relevant, those in vivo investigations may not be able to fully mimic all aspects of the human scenario underlining a variability between animal models and humans [10]. The complexity of the pathology, the imperfection of existing models and ethical issues make mandatory the identification of alternative models able to closely mimic the critical aspects of fibrosis as a platform to test novel pharmaceutical therapies for still uncurable conditions.

A good compromise to overcome the important limits of 2D cultures and animal models is the use of the engineered 3D tissues [10]. Currently, several types of advanced 3D cultures have been proposed such as self-assembled models (spheroids and organoids), biofabricated systems, organ derived cultures or cells growth in bioreactor or chips [10]. The 3D fibrosis modeling may offer relevant advantages to reproduce the spatial organization of fibrotic microenvironment and compartmentalization allowing the possibility to study crucial pattern formed, as example, by collagen deposition and tissue stiffness. In this framework, an important role could be played by bioprinting, as relatively recent technology to print tissues and organs through layer-by-layer deposition of viable cells, biomaterials and biological molecules [18].

We here propose a novel biomimetic model able to recapitulate the abnormal fibroblast potential to reorganize the ECM by a synergic TGFβ/type I collagen stimulation. Providing a highly physiological ex vivo human tissue model we have been able to closely mimic fibrotic tissue organization and composition in a standardized manner to be tested by anti-fibrotic agents. So far, few drugs have been recommended by regulatory agencies for fibrosis: nintedanib and pirfenidone. Although these options are used worldwide, their mechanism of action is yet poorly understood [17]. Thus, by this bioprinted model we are proposing a new platform for better disease understanding and as a promising tool for drug testing in fibrosis.

2. Material and methods

2.1. Cell Cultures

2.1.1. Standard 2D cell culture

Primary human foreskin fibroblasts (HFFs; American Type Culture Collection ATCC, Manassas, VE, USA) were seeded according to manufacturer instructions at a density of 8000 cells/cm^2 in Dulbecco's modified Eagle's medium (DMEM, Gibco, BleiswijK, the Netherlands) containing 15% Fetal Bovine Serum (FBS, Euroclone, Pero, Italy), 1% Penicillin/Streptomicin (Gibco, Grand Island, NY, USA) and 2% Glutamine (Gibco, Grand Island, NY, USA). When confluence was reached, cells were detached with 0.05%/0.02% Trypsin/EDTA (Gibco, Paisley, UK) at 37 °C/5% CO_2, quantified by trypan blue 0.4%, (Sigma, St Louis, MO, USA) and then seeded at the density adequate for each analysis. Independently from the analysis performed, 2D cell cultures were starved for 18 h culturing with medium containing 2.5% Nuserum (Corning, Bedford, MA, USA), 1% Penicillin/Streptomicin (Gibco), 2% glutamine (Gibco) in DMEM (Gibco) and then stimulated with TGFβ (10 ng/ml, Peprotech, London, UK), type I collagen (40 μg/ml, Corning, Bedford, MA, USA) or a mix of TGFβ (10 ng/ml) and type I collagen (40 μg/ml; Corning) for 72 h. Cell morphology was observed by microscopical analysis by contrast microscopy with and EVOS FL Cell Imaging System (Thermo Fisher Scientific).

2.2. 3D printing

Bioprinting process was performed by using a commercial 3D printer (3D Bioplotter®, EnvisionTEC, Gladbeck, Germany) under sterile flow hood cabinet. The bioink is composed by (i) highly concentrated type I collagen (Lifeink® 200, Advanced BioMatrix, San Diego, CA, USA, 35 mg/ml) and (ii) HFF cells dispersed in a suitable medium (DMEM + 10% FBS + 2% L-glutamine + 1% penicillin/streptomycin) at the concentration of 2.3 × 10^6 cells per ml of ink. Collagen and cell-laden medium were mixed in a volume ratio of 5:1 and the bioink was carefully loaded in a 30 ml cartridge (Nordson, Westlake, OH, USA) fitted with a conical needle (25 G, Nordson). The syringe was connected to the low temperature printing head and kept at 4 °C throughout the process. A customized CAD (customized aided design) project was realized to print the bioink in the form of a cylinder 960 μm high, with a diameter of 8 mm, a slicing height of 240 μm and composed by 4 layers.

The bioprinting was performed using pneumatic pressure of 0.7 bars and printing speed of 7 mm/s. The process was conducted in liquid environment, by extruding the ink into a plastic plate placed on the printing platform and filled with culture medium at about 37 °C. Therefore, after printing, the scaffolds were left at 37 °C for at least 30 min and then transferred to the incubator to provide adequate cell culture conditions (37 °C, 5% CO2).

3D models were cultured in DMEM containing 10% FBS, 1% Penicillin/Streptomicin and 2% Glutamine for 72 h at 37 °C /5%CO_2. After 18 h of starvation with medium containing 2.5% Nuserum, 1% Penicillin /Streptomicin, 2% glutamine in DMEM, the profibrotic stimulus TGFβ was added at the concentration of 10 ng/ml for 72 h. After stimulation, 3D models were processed for analysis described below.

To study the ability of 3D models to serve as platform for drug testing, samples were co-stimulated by TGFβ with/without the anti-fibrotic drug nintedanib (0,1 μM, 1 μM and 10 μM, Sigma Aldrich) or pirfenidone (100 μM, 500 μM and 1000 μM, Sigma Aldrich). DMSO treated samples were used as negative controls. After 72 h, the effects of the drugs were checked in terms of viability, fibronectin expression, SEM analysis and Picrius Sirius Red staining.

2.3. Immunofluorescence

HFF were plated into multiwell 12 at a density of 8000 cells/cm^2 and stimulated as previously described. 72 h from stimuli administration, cells were washed in PBS 1X and fixed in situ in 4% formaldehyde (Histo-Line, MI, Italy) for 20 min. After washing in PBS, cells were permeabilizated by incubation for 3 min with 0.5% Triton X-100 (Sigma, St Louis, Mo. USA) on ice and then incubated for 30 min with 0.1% bovine serum albumin (Sigma St Louis, MO, USA), 10% normal goat serum (Vector, Burlingame, CA, USA) and 60 min with the primary antibodies rabbit pAb αSMA (1:75, ab5694, Cambridge, UK) or rabbit pAb fibronectin (1:200, ab2413, Abcam). After 3 washes in PBS, cells were incubated for 1 h at room temperature with donkey anti rabbit Dylight 594 (Bethyl Laboratoires, Montgomery, TX, USA). Nuclei were counterstained with DAPI (Thermo Fisher Scientific, Eugene, OR, USA) for 5 min at room temperature. Fluorescent cells were observed by AxioZoom V16 (Zeiss) and by AxioImager M2 (Zeiss) for 2D and 3D models respectively.

2.4. Phalloydin staining

To stain F-actin fibers, Dylight 594-Phalloydin (Thermo Fisher Scientific), 2D and 3D models were fixed in 4% formaldehyde for 20 min and then incubated in the dark with the dye at the concentration of 1IU/ml for 40 min at room temperature. After 3 washes in PBS, nuclei were counterstained with DAPI for 5 min at room temperature. Images were acquired by AxioZoom V16 (Zeiss) and by AxioImager M2 (Zeiss) for 2D and 3D models respectively.

2.5. Fibroblast migration assay

A total of 200′000 HFF were plated on 12 well tissue culture plates until confluence reaching. Subsequently, the cells were washed with sterile PBS and a scratch for each well were drawn along the cell monolayer with a sterile plastic tip. Cells were washed three times with PBS to remove all detached cells and incubated with HFF medium containing TGFβ (10 ng/ml), type I collagen (40 μg/ml) or a mix of TGFβ

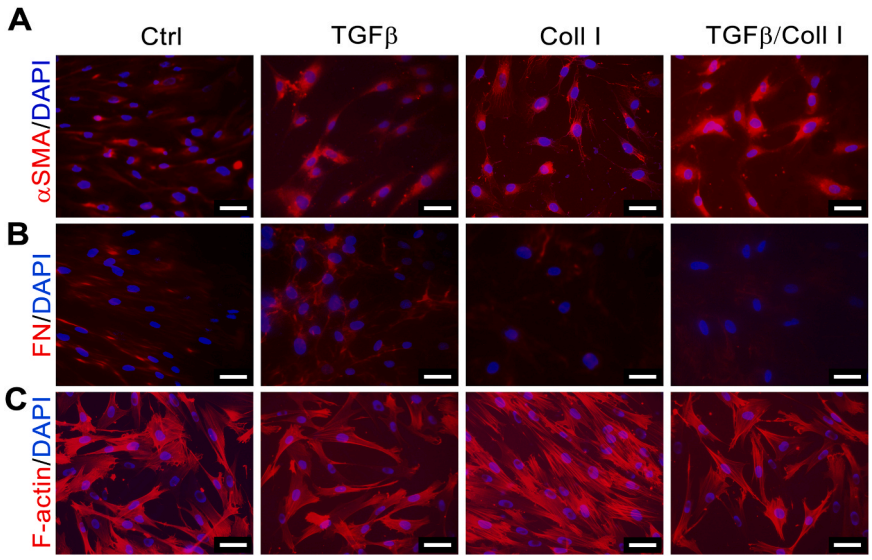

Fig. 1. Characterization of normal human healthy fibroblasts under stimulation by TGFβ and type I collagen (alone or in combination). Specific immunofluorescence staining for (A) alpha Smooth Muscle Actin (αSMA), (B) fibronectin (FN) and (C) and F-actin. DAPI (blue) was used as counterstaining for cell nuclei. Bar= 50 μm.

(10 ng/ml) and type I collagen (40 μg/ml). After 24 h, cells were fixed with 4% formaldehyde and stained with Cristal Violet (0.4%, Sigma Aldrich) for 20 min at room temperature. Migrated cells were observed by Axio Observer.Z1 (Zeiss)), counted from three different area. Results were expressed as the mean ± standard deviation and reported to negative control (100%).

3. Live/dead

LIVE/DEAD staining was performed by using LIVE/DEAD Cell viability/cytotoxicity assay kit (ThermoFisher Scientific). Briefly, 3D cultures were stained with 500 μL of the LIVE/DEAD solution containing 2 μM calcein AM and 4 μM EthD-1 and incubated for 45 min at 37 °C/5% CO_2. After staining, 3D models were rinsed in PBS and immediately analyzed using Axio Zoom V16 (Zeiss).

3.1. Picrius sirius red

3D models were fixed in 2.5% glutaraldehyde solution, dehydrated in ascendent alcoholic scale and paraffin embedded. Four μm–thick sections were stained for 1 h with a 0.1% solution of Direct Red (Sigma Aldrich) in saturated aqueous picric acid (Sigma Aldrich) and washed in 0.5% Acetic Acid (Carlo Erba). Slides were then dehydrated through ascending alcohols, cleared in xylene and mounted. Picrosirius red–positive areas were visualized under brightfield and circular polarized light in order to discriminate red and yellow-green fibers in 5 randomly chosen fields using AxioZoom V16 (Zeiss). Quantification was performed by Image analysis plugin (ZEN Pro, Zeiss). Positive area was expressed as percentage and normalized with untreated control (considered as 100%) or with TGF-treated samples in test with drugs.

3.2. SEM analysis

3D models were rinsed in PBS, fixed for in 4% Paraformaldehyde with 2% Glutaraldehyde overnight, dehydrated in an ascending ethanol series (50%, 70%, 90%, 100% (twice); 15 min each) and immersed in 1 ml of hexamethyldisilazane for 10 min (twice), before overnight drying for 10 h.

Samples are mounted on SEM stub with a conductive carbon tape and are sputtered with Gold/Palladium target in order to enhance the samples conductivity.

SEM Analysis was performed by Scanning Electron Microscope SEM TM4000 II plus Mot 55E-0312 – Hitachi. Surface micrographs were acquired with an acceleration electron beam of 5 kV, medium vacuum mode, with secondary electron mode (SE) and 30x, 120x and 600x of magnification.

3.3. Statistical analyses

For fibroblast migration assay, results were analyzed by Student's t test obtaining a p-values referred to the mean comparison between treated cells and unstimulated control. P value < 0.05 (*) and < 0.001 (**) were considered statistically significant. In Picrius Sirius Red staining, significance was set at $p < 0.05$ (*) and $p < 0.01$ (**). Data are expressed as means ± standard deviations (SD).

4. Results

4.1. TGFβ and type I collagen promote fibrotic features

The cytoskeletal protein αSMA is a pivotal myofibroblast marker [7,19]. Therefore, focusing on αSMA, we began assessing in standard 2D culture whether dermal fibroblasts could be stimulated with TGFβ and/or type I collagen or both. As visible in Fig. 1A, we observed a strong increase in αSMA expression compared with untreated cells. In addition, intensity signal αSMA protein was mostly detected when TGFβ and type I collagen were simultaneously added to the culture.

More we focused on fibronectin, as one of the most abundant proteins secreted during fibrosis [20], uncovering that the addition of the profibrotic factor TGFβ have slightly increased in the fibronectin expression (Fig. 1B). Surprisingly, fibronectin was almost absent in cells receiving type I collagen alone or in combination with TGFβ.

We then focused on F-actin, a known marker of cytoskeleton [21], identifying a rearranged apparatus in all conditions. In particular, when collagen I was added into the culture media (alone or in combination with the TGFβ), F-actin reorganized the cytoskeleton in a visible actin stress bundle fiber (Fig. 1C). These data indicate that TGFβand type I collagen are pivotal and synergic drivers in fibrosis biomimesis.

4.2. TGFβ induces nodule formation

Migratory ability is a crucial aspect in the early phase of the pathogenesis of fibrosis [22]. In order to establish the potential of type I collagen and TGFβ (alone or in combination) to influence migration of

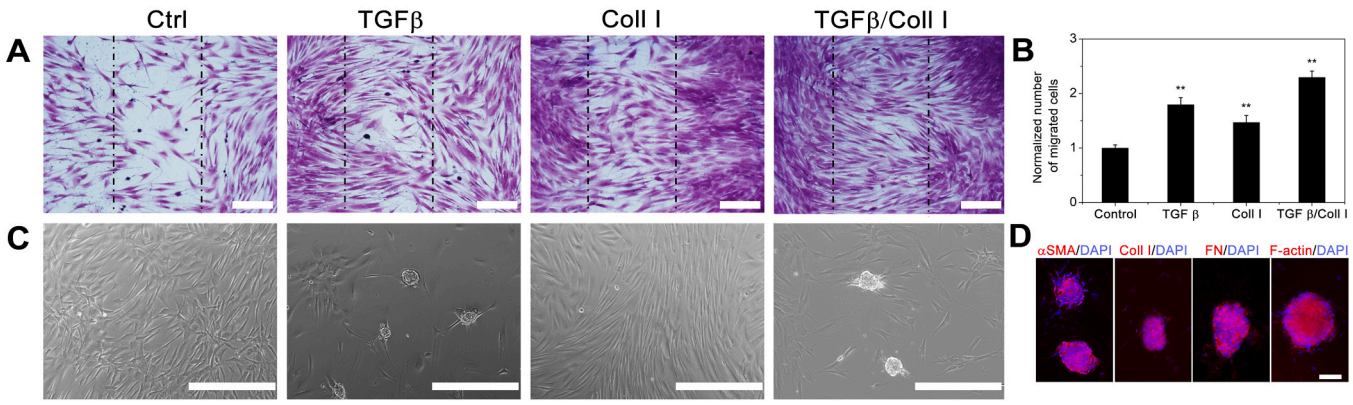

Fig. 2. Fibrotic behavior of normal human healthy fibroblasts after 24 h of stimulation by TGFβ and type I collagen (alone or in combination). (A) Representative photomicrographs of migration assay after Crystal Violet staining. The dashed lines represent the leading edges. Bar 100 μm. (B) Quantification of migrated cells from three different area. P value < 0.05 (*) and < 0.001 (**) were considered statistically significant. (C) Spontaneous nodule formation after exposition to TGFβ, type I collagen (alone or in combination) for 24 h. Bar= 1000 μm. (D) Immunofluorescence staining of alpha Smooth Muscle Actin (αSMA), type I collagen (Coll I), fibronectin (FN) and F-actin. Bar= 50 μm.

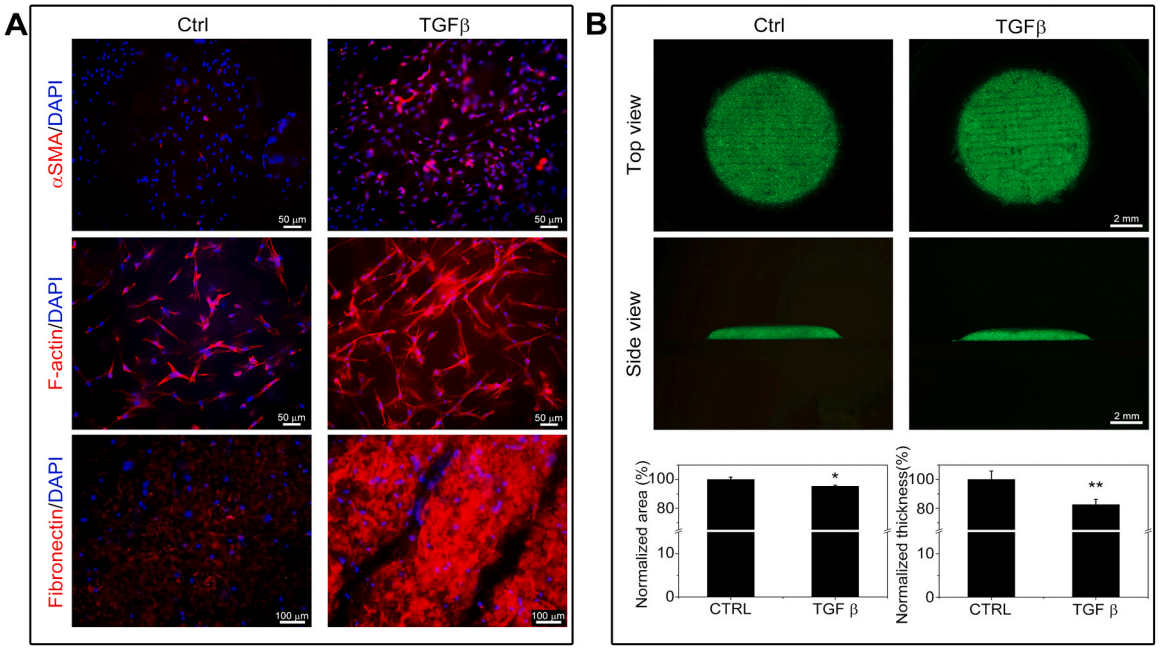

Fig. 3. Characterization of 3D models obtained by bioprinting after TGFβ stimulation. Immunofluorescence staining for alpha Smooth Muscle Actin (αSMA), F-actin and fibronectin expression. Nuclei were counterstained with DAPI. Bar= 50 μm (A). (A) Microscopical observation of LIVE/DEAD staining through XY (top view) and (B) Z axis (side view). Bar= 2 mm. Quantification of area and thickness of 3D models.

dermal fibroblasts, scratch assay was performed in 2D standard model (Fig. 2 A and B). After 24 h from administration, all stimulated fibroblasts showed a tendency towards increased migration in a statistically significant manner (p-value < 0.01, Fig. 2B). Migratory behavior of TGFβ and type I collagen stimulated cells was respectively of 1.8 ± 0.13-fold and 1.5 ± 0.13-fold higher if compared with control. The synergic activity of TGFβ and type I collagen strongly potentiated the chemotactic activity of fibroblasts reaching a migration rate of 2.3 ± 0.12-fold higher than unstimulated cells (Fig. 2B).

Surprisingly, nodule like aggregates were precociously observed at 24 h in TGFβ alone or in combination with type I collagen stimulated cells. Nodule formation was not detected in control and in type I collagen stimulated fibroblasts (Fig. 2 C). To better characterize the nature of the newformed 3D structures, an immunofluorescence assay was performed revealing that nodules showed a marked positivity for F-actin and αSMA, and confirming the fibroblastic nature of nodule forming cells. In addition, nodules demonstrated an enriched of ECM specific proteins as fibronectin and type I collagen, (Fig. 2D), collectively suggesting that fibrotic nodule formation is directly correlated with TGFβ.

4.3. TGFβ stimulates the remodeling of 3D models

Having established that the synergic action of both type I collagen and TGFβ to potentiate the fibrotic behavior in a 2D approach, we then designed a new 3D model based on bioprinting technology, where type I collagen was bioprinted and TGFβ was added in the culture medium. After bioprinting, LIVE/DEAD assay was performed and fibroblasts within the scaffold resulted viable and homogeneously distributed (data not shown).

In order to investigate the behavior of the cells embedded within 3D matrix, we analyzed the expression of F-actin, αSMA and fibronectin

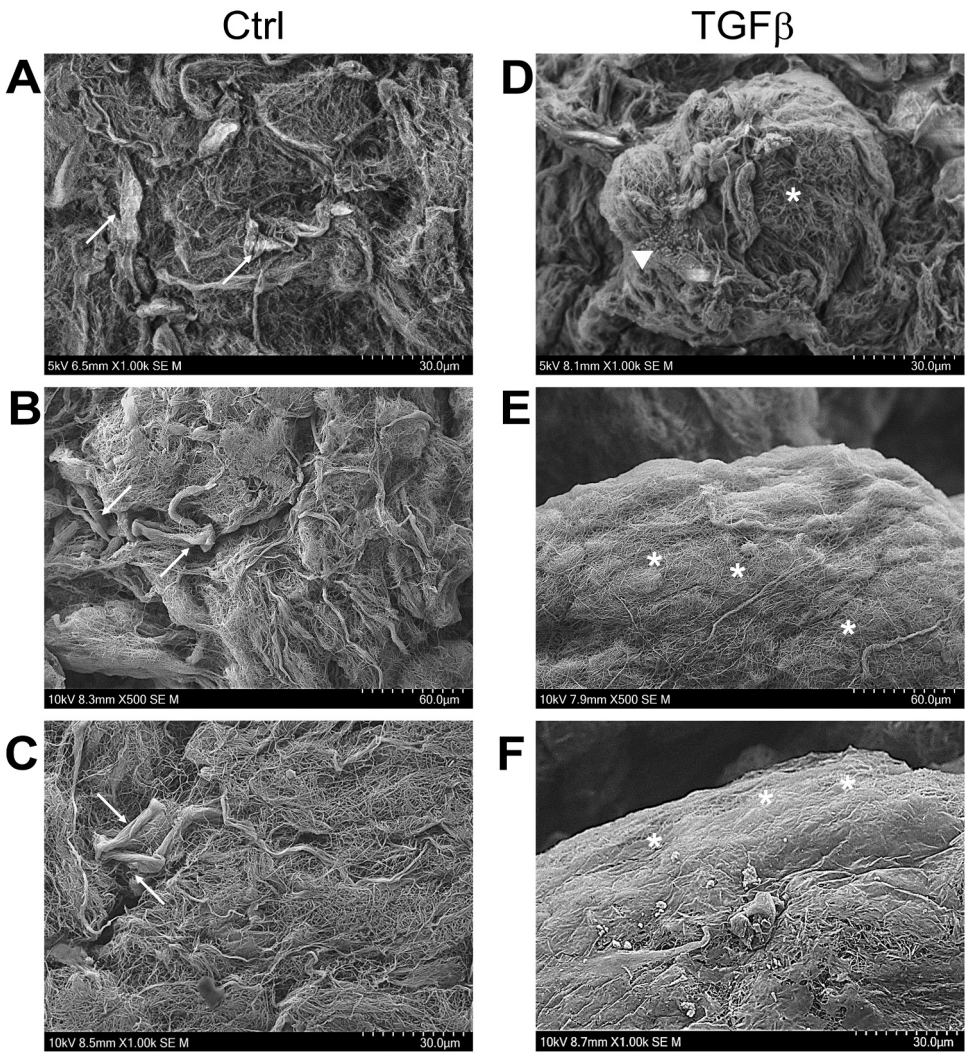

Fig. 4. Scanning Electron Microscopy (SEM) analysis of 3D model. Representative microghraps of (A, B, C) negative control and (D, E, F) model after stimulation with TGFβ. Bar: 30 and 60 μm.

proteins by immunofluorescence staining. F-actin and αSMA, both involved in cytoskeleton reorganization and matrix contraction, strongly increased after TGFβ stimulation. In addition, the administration of TGFβ dramatically increased the expression of fibronectin, as most abundant protein secreted during fibroplasia [20] (Fig. 3A). All together, these data suggest that 3D model is able to recapitulate key features of fibrosis.

Microscopical observation of LIVE/DEAD staining through XY and Z axis (as top and side view respectively, reported in Fig. 3B) surprisingly revealed that untreated samples and TGFβ stimulated scaffolds reached different size. The values of area and thickness of treated samples was respectively of $5 \pm 0.7\%$ and $17.4 \pm 3.6\%$ lower than unstimulated model (p value < 0.05 for area and p value < 0.01 for thickness, Fig. 3B, bottom panel).

The microarchitecture of the scaffold was then explored by SEM analysis after 72 h post stimulation (Fig. 4). Untreated model showed the presence of visible elongated fibroblasts interacting with bioink collagen fibers, as indicated in Fig. 4A, B and C (arrows heads). On the contrary, TGFβ stimulated the remodeling ability of fibroblasts. Formation of fibrotic noduli characterized by the presence of neo-formed fibrillar structures (Fig. 4D and E, asterisks) and microvilli (Fig. 4D, arrow heads) was observed. In addition, the stimulation of the scaffold with TGFβ strongly increased the deposition of ECM which covers large areas of the 3D model, as reported in Fig. 4F. The scaffold surface appeared denser and more compact if compared with untreated samples, as reported in Figs. 4E and 4F.

The collagen pattern of the 3D model was further investigated by Picrius Sirius Red staining (Fig. 5). By brightfield observation, TGFβ stimulated sample revealed a more compact and rearranged structure, in comparison with control, as suggested by a darker red staining (Fig. 5A, upper panel). Polarized light observation confirmed that TGFβ administration strongly increased the presence and the intensity of green, red and yellow fibers (Fig. 5A, bottom panel). This finding has been then confirmed by signal quantification revealing that collagen pattern in stimulated samples was 20-fold higher as compared to untreated controls, in a statistically significant manner (p value>0.019, Fig. 5B). Collectively, we have developed an in vitro 3D model of fibrosis where TGFβ and type I collagen promote fibrogenesis and sustain a progressive accumulation of ECM and microarchitecture remodeling.

4.4. The 3D model of fibrosis as platform for drug testing

The bioprinted model was then tested for responsiveness to the two market-approved antifibrotic drugs, nintedanib or pirfenidone, administered during stimulation with TGFβ.

After 72 h of treatment, the Live and Dead staining revealed that the lower doses of nintedanib (0,1 μM and 1000 μM) did not impact on cell viability. On the contrary, the highest dose (10 μM) strongly inhibited

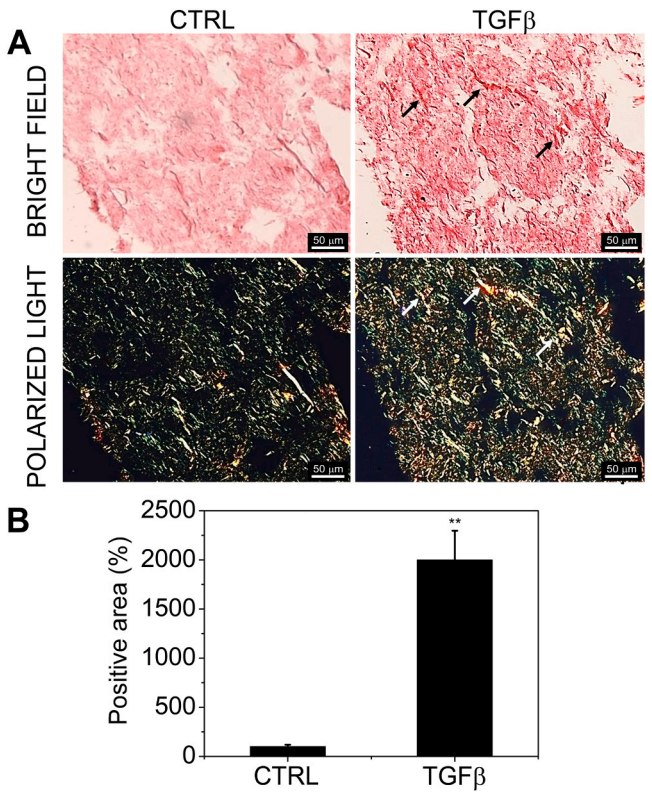

Fig. 5. Analysis of collagen fibers after Picrius Sirius Red staining of 3D model with or without TGFβ stimulation. (A) Sirius Red stained sections were analyzed by brightfield (upper panel) and polarized light microscopy (bottom panel). Bar: 50 μm. (B) Picrius Sirius Red positive collagen fibers were quantified by Image Analysis (Zen). Significance was set at $p < 0.05$ (*) and $p < 0.01$ (**).

the cell viability. The overall cell survival was not affected when the models were stimulated by pirfenidone, at all tested doses (Fig. 6A).

To test the potential of the model to highlight the effect of the drugs on cytoskeleton rearrangement, phalloidin staining was performed. As reported in Fig. 6B, TGFβ alone strongly stimulated the cytoskeleton reorganization. On the contrary, when TGFβ was administered in presence of both the antifibrotic drugs as single agent, the F- actin reorganization was inhibited in a dose dependent manner.

In parallel, we studied the effect of nintedanib and pirfenidone on ECM remodelling. The immunofluorescence staining for fibronectin, revealed that the overexpression of the protein induced by TGFβ was strongly reduced in presence of antifibrotic drugs. The reduced levels of fibronectin in nintedanib-treated samples appeared dose-dependent. The best effects of pirfenidone in inhibiting or slowing down the deposition of fibronectin were detected with the highest dose 500 μM and 1000 μM (Fig. 7A).

To better study the effects of the drugs on ECM, the microarchitecture of the scaffold was analyzed by SEM. In TGFβ stimulated samples, collagen fibers organized themselves in bundles and ECM neodeposition was visible (arrows). On contrary, after stimulation with the anti-fibrotic drugs, the phenotype of the scaffold was reverted: no ECM deposition was detected and collagen fibers appeared individually arranged and not aggregated in bundle, supporting the anti-fibrotic potential of the drugs (Fig. 7B).

To explore the role of the drugs in collagen pattern, specimens were stained by Picrius Sirius Red. Both nintedanib and pirfenidone was able to inhibit the collagen deposition promoted by TGFβ as reported in Fig. 7C, showing a decreased red signal in stimulated samples. Significant results were confirmed by positive signal quantification: when nintedanib was used at the dose of 1 μM and 10 μM, we detected a collagen positivity of $59,29 \pm 8,26\%$ and $54,88 \pm 8,15\%$ in a statistically significant manner (p value < 0.001). Not significant differences were observed when nintedanib was used at lower dose (0.1 μM). A similar trend was observed after pirfenidone treatment: for each dose used we observed a dose dependent reduction in picrius sirius red positivity, registering a positivity of $38,82 \pm 5,65\%$, $28,06 \pm 4,38\%$ and $27,71 \pm 6,88\%$ (respectively for 100 μM, 500 μM and 1000 μM of pirfenidone) in comparison with TGFβ treated sample.

These results, confirming the already established knowledge of the potential of nintedanib and pirfenidone in the treatment of fibrosis, support the ability of the bioprinted model to emphasize how fibrosis could impact on tissue reorganization and to predict if a putative clinical treatment could revert pathological features.

5. Discussion

The term "fibrosis" refers to a final outcome of several pathological conditions affecting various tissues and organs [1]. At the cellular level, the central mediators of fibrosis are fibroblasts, an heterogenous cell population, able to transdifferentiate in myofibroblasts, mechanically active cells equipped with a well-developed contractile apparatus [19]. αSMA is historically considered as a biochemical marker of myofibroblasts [23,24], being involved in the formation of robust actin stress fibers, ECM remodeling and consequently, in the hardening and/or scarring of injured tissues [1,2].

To date, the most frequent tools used to investigate the basis of the pathological mechanisms of fibrosis are in vitro 2D cellular approaches. In the present work, we started from a 2D model in which normal human healthy fibroblasts were stimulated by TGFβ, type I collagen or both. The transdifferentiation of fibroblast into myofibroblast, occurring after stimulation with TGFβ, was confirmed by the overexpression of the αSMA protein and the creation of a contractile apparatus with large bundles of F-actin microfilaments.

Fibroblast migration is one of the earlier steps in fibrosis pathogenesis and it is responsible for expansion of fibrotic lesions, formation of cellular aggregates also known as the "leading edge", and ultimately scar formation [25,26]. In our 2D model, the administration of key fibrotic factors TGFβ and type I collagen to cell culture, increased the chemotactic potential of fibroblast in a statistically significant manner, in particular when the stimuli were administered in combination. Curiously, after stimulation with TGFβ (alone or in combination with type I collagen), we observed a dual scenario: fibroblasts normally adhering in 2D monolayer and, occasionally, fibroblasts spontaneously organizing in 3D structures, as also reported by Qihe Xu et al. [27]. Authors observed that TGFβ stimulation for 24 and 48 h rapidly promotes ECM enriched nodule formation. The process occurred in 2D culture of fibroblast isolated from several sources (kidney, lung, spleen, skin) and was described as a highly dynamic event. In that context cells migrated from one nodule to the other, with the same nodules merging into a larger structure, supporting that a 3D architecture favor a more prominent chemotactic potential and a higher ECM deposition [27].

Given that the strong upregulation of ECM is the crucial event in fibrosis [28], we focused on fibronectin deposition in monolayer and in 3D aggregates. We detected high level of fibronectin staining when normally adherent fibroblasts were stimulated by TGFβ. On the contrary, the presence of type I collagen in the medium culture did not determine the expression of fibronectin specific signal. Focusing on the 3D small aggregates of fibroblasts forming during 2D cell cultures, we observed high levels of expression of αSMA, and ECM proteins fibronectin and type I collagen. This finding is supported by literature where described nodules are enriched of ECM [27] and are proposed as in vitro assay to mimic the "leading edge" observed in fibrosis affected patients as results of unstoppable fibrotic response [25]. Unfortunately, the aggregation of fibroblasts in 3D structures was a random event not occurring in all experiment performed. In addition, the ambiguous behavior observed in the same plate when fibroblasts are in form of monolayer or organized in 3D aggregates highlight the crucial limit of

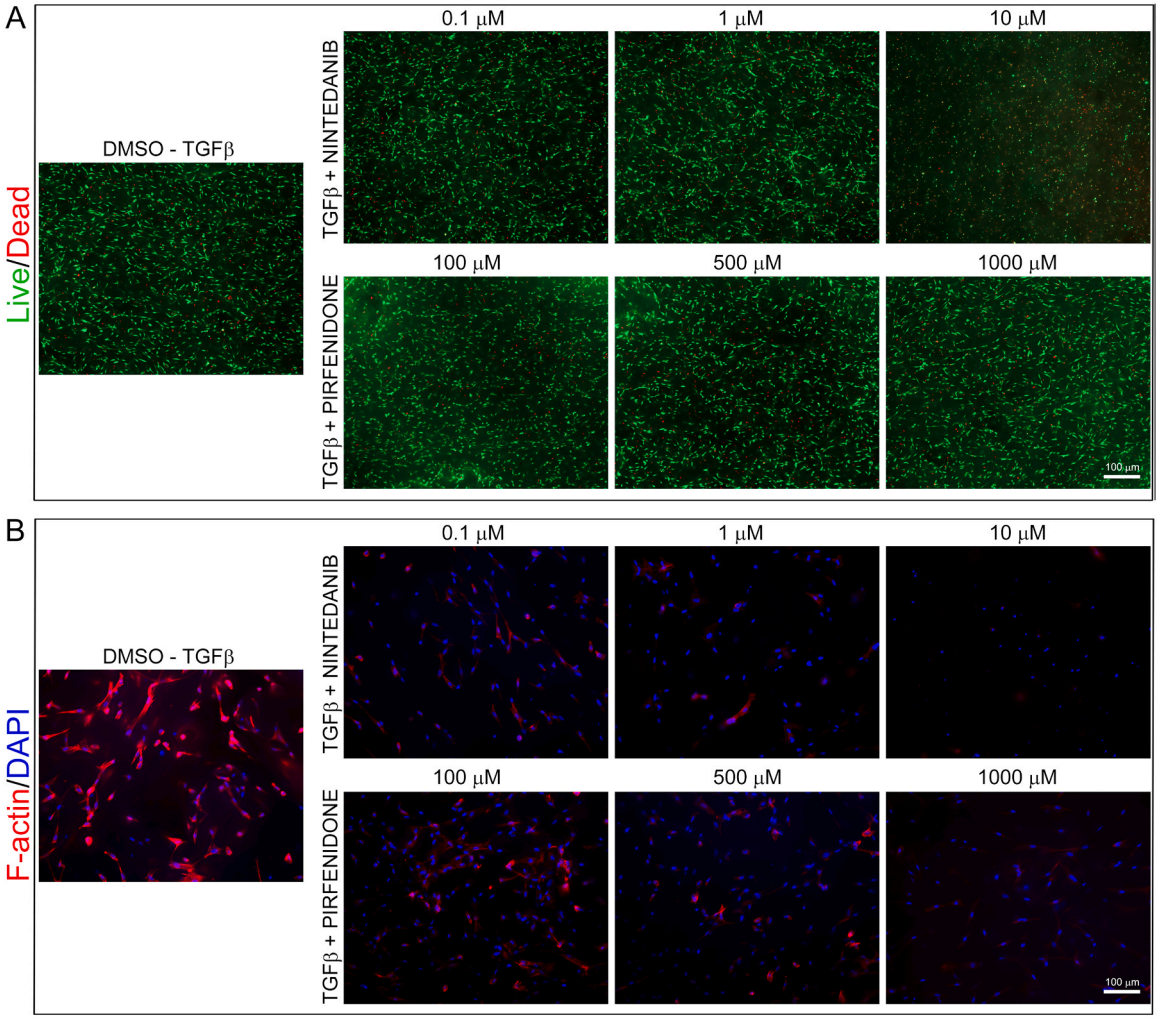

Fig. 6. Effects of nintedanib and pirfenidone treatment on the fibrotic phenotype of 3D model. (A) Microscopical observation of LIVE/DEAD staining. Bar= 100 μm. (B) F-actin expression. Nuclei were counterstained with DAPI. Bar= 100 μm.

2D adherent cells system that is the inability to reproduce physiological 3D tissue environment and to mimic tridimensional spatial organization, cell-cell/cell-matrix interaction and the role of ECM. On the other hand, none of the current available animal models of fibrosis are able to reproduce the complexity of the pathology given the large differences between animal and human. In addition, the growing ethical issues make mandatory the identification of alternative models able to closely mimic the critical features of fibrosis.

In order to overcome these shortcomings, we fabricated a 3D model by bioprinting technology. In detail, high concentrated type I collagen was mixed with fibroblasts and TGFβ was administered to culture medium to promote the transdifferentiation into myofibroblasts.

We found that TGFβ stimulation strongly increased αSMA and F-actin expression suggesting cytoskeleton reassembly and the formation of large stress fibers as fibrotic features [19].

The high levels of fibronectin detected after TGFβ stimulation, is an important advancement of the model. In fact, the 2D approach failed to enhance the expression of fibronectin during collagen stimulation, enhancing the crucial importance of the 3D microenvironment. The major predictivity of 3D systems is conferred by the detection of high levels of fibronectin expression (and so matrix neodeposition) after collagen and TGFβ costimulation, in contrast of 2D results where the presence of type I collagen inhibits the fibronectin secretion.

To further confirm the ability of the model to impact on the collagen network, Picrius Sirius Red staining was performed. The dye, specifically binding to collagen fibrils, revealed that 3D models dramatically increased the synthesis of collagen and then, the abnormal deposition of ECM.

The ability of the 3D model to better recapitulate tissue architecture, the cell-matrix interaction and the delicate role of ECM was macroscopically evident. We observed a strong reduction of the thickness of TGFβ stimulated model. This finding may be due to a greater contractive capacity of treated fibroblasts which acquired high cytoskeleton reassembly given the high levels of F actin and αSMA expression after TGFβ stimulation [19].

These features make our 3D bioprinted model a suitable biomimetic model in which cells can self-assembly in a 3D construct and reconstitute in vitro a fibrotic condition under TGFβ and type I collagen stimulation. The identification of new therapeutic strategies to fight fibrosis is an urgent need in clinical scenario: only two drugs are recommended for the treatment of fibrosis: nintedanib and pirfenidone. Currently, no drugs are able to revert the pathological conditions: nintedanib and pirfenidone only slow down the progression of pulmonary fibrosis [17].

To evaluate the ability of the bioprinted 3D model to serve as a platform for drug screening, nintedanib and pirfenidone were administered in presence of TGFβ at three different concentrations. After 72 h of stimulation, the platform was able to highlight the therapeutic action of the drugs, emphasizing the ability of the model to show the change in cytoskeleton organization, in ECM deposition, in architecture remodeling and in collagen network, as response to drug.

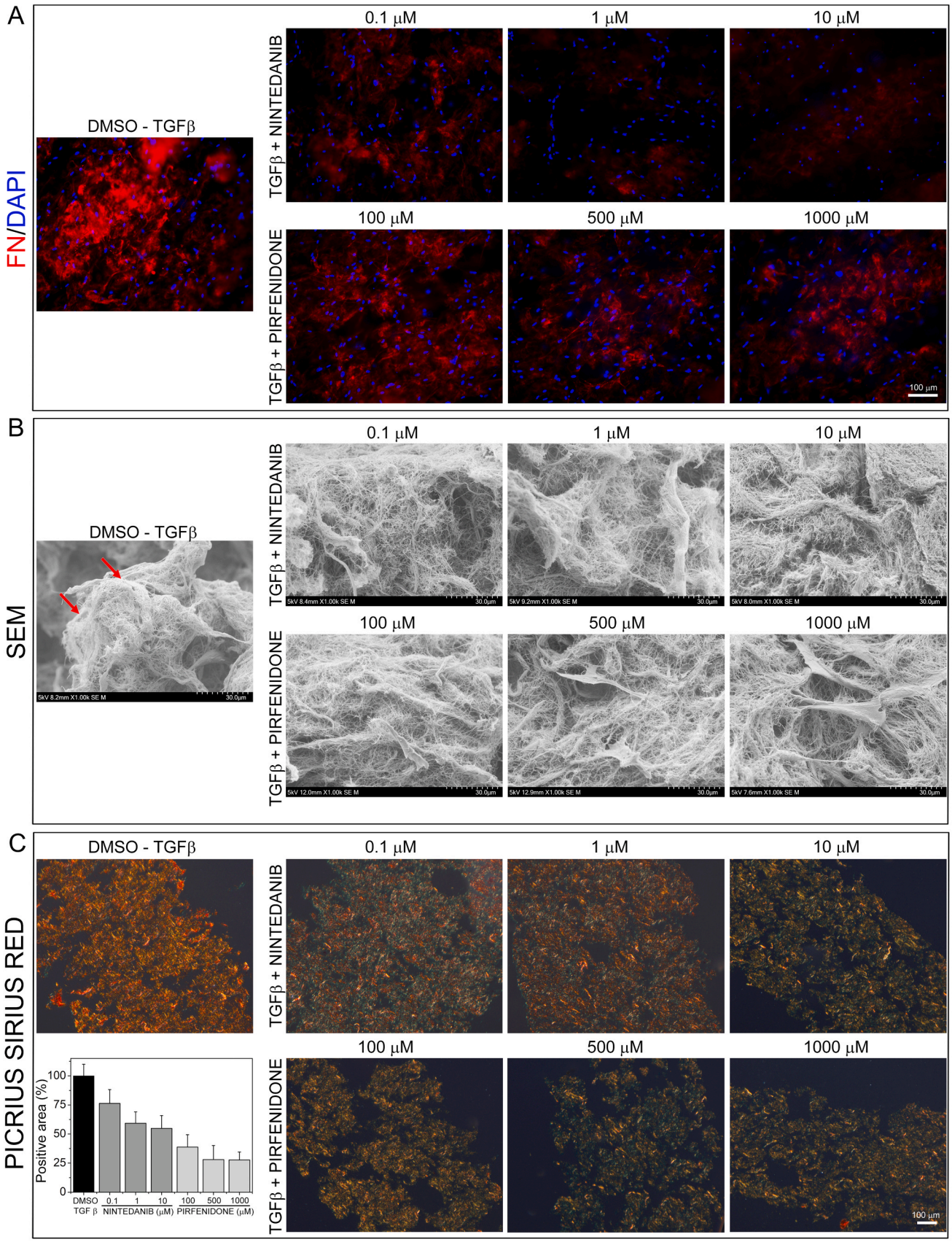

Fig. 7. Effects of nintedanib and pirfenidone treatment on fibrotic ECM remodeling. (A) Immunofluorescence staining of fibronectin (FN). Nuclei were counter-stained with DAPI. Bar= 100 μm. (B) Scanning Electron Microscopy (SEM) analysis of 3D model. Bar= 30 μm. (C) Analysis of collagen fibers after Picrius Sirius Red by polarized light microscopy. Bar = 100 μm.

Thus, this biomimetic model could be useful to study fibrotic disorders involved not also skin but it could be extended to the study of all fibrotic organs by introducing tissue specific fibroblasts and investigations are currently ongoing for kidney and lungs. In addition, the use of healthy tissues-derived fibroblasts, even not terminally differentiated, allow to study the initial phases of fibrosis. In conclusion, the ability to synthetize a bioprinted 3D model by an automated, standardized and reproducible manner, will provide a novel platform for a more reliable fibrosis understanding and for innovative drug discovery against a still lethal condition affecting a variety of human diseases.

CRediT authorship contribution statement

Tiziana Petrachi: Conceptualization, writing of original draft. **Alberto Portone:** Investigation. **Gaelle Francoise Arnaud:** Validation. **Francesco Ganzerli:** Investigation. **Valentina Bergamini:** Visualization. **Elisa Resca:** Data curation. **Luca Accorsi:** Methodology. **Alberto Ferrari:** Formal Analysis. **Annalisa Delnevo:** Resources. **Luigi Rovati:** Software. **Chiara Chiavelli:** Writing, review and editing. **Massimo Dominici:** Funding acquisition, Supervision, Writing, review and editing. **Elena Veronesi:** Project Administration, Supervision.

Declaration of Competing Interest

The authors declare that they have no known competing financial interests or personal relationships that could have appeared to influence the work reported in this paper. Tiziana Petrachi, Alberto Portone, Gaelle Francoise Arnaud, Francesco Ganzerli, Valentina Bergamini, Elisa Resca, Luca Accorsi, Alberto Ferrari, Annalisa Delnevo, Luigi Rovati, Caterina Marra, Chiara Chiavelli, Massimo Dominici and Elena Veronesi DECLARE NO competing financial interests or personal relationships that could have appeared to influence the work reported in this paper.

Data Availability

Data will be made available on request.

Aknowledgment

We are grateful to the Fondazione Democenter-Sipe for the contribution to this research. The research leading to these results was partially funded by the project POR FESR 2014–2020 (CUBIBOX: Customized Biological Box. Piattaforma di nuova generazione per testing in vitro) and by “Progetti Dipartimenti Eccellenti MIUR 2017″.

Brief Commentary

Background: To date, the most frequent tools used to investigate the pathological mechanisms of fibrosis are in vitro 2D cellular approaches, lacking for complexity. On the other hand, none of the current available animal models are able to recapitulate human fibrotic features. The identification of new platform for study fibrosis and test the drug efficacy is mandatory.

Translational significance: The described 3D model is able to mimic fibrotic features recapitulating the abnormal fibroblast potential to reorganize extracellular matrix. The model provides a novel platform for a more reliable fibrosis understanding and for innovative drug discovery against fibrosis.

References

[1] D.C. Rockey, P.D. Bell, J.A. Hill, Fibrosis–a common pathway to organ injury and failure, N. Engl. J. Med. 372 (2015) 1138–1149, https://doi.org/10.1056/NEJMra1300575.

[2] N.C. Henderson, F. Rieder, T.A. Wynn, Fibrosis: from mechanisms to medicines, Nature 587 (2020) 555–566, https://doi.org/10.1038/s41586-020-2938-9.

[3] M. Sato, Y. Muragaki, S. Saika, A.B. Roberts, A. Ooshima, Targeted disruption of TGF-Beta1/Smad3 signaling protects against renal tubulointerstitial fibrosis induced by unilateral ureteral obstruction, J. Clin. Invest. 112 (2003) 1486–1494, https://doi.org/10.1172/JCI19270.

[4] W.A. Border, N.A. Noble, Transforming growth factor beta in tissue fibrosis, N. Engl. J. Med. 331 (1994) 1286–1292, https://doi.org/10.1056/NEJM199411103311907.

[5] D.E. Clouthier, S.A. Comerford, R.E. Hammer, Hepatic fibrosis, glomerulosclerosis, and a lipodystrophy-like syndrome in PEPCK-TGF-Beta1 transgenic mice, J. Clin. Invest. 100 (1997) 2697–2713, https://doi.org/10.1172/JCI119815.

[6] P.J. Sime, Z. Xing, F.L. Graham, K.G. Csaky, J. Gauldie, Adenovector-mediated gene transfer of active transforming growth factor-beta1 induces prolonged severe fibrosis in rat lung, J. Clin. Invest. 100 (1997) 768–776, https://doi.org/10.1172/JCI119590.

[7] A. Vallée, Y. Lecarpentier, TGF-β in fibrosis by acting as a conductor for contractile properties of myofibroblasts, Cell Biosci. 9 (2019) 98, https://doi.org/10.1186/s13578-019-0362-3.

[8] R.A.F. Clark, G.A. McCoy, J.M. Folkvord, J.M. McPherson, TGF-B1 stimulates cultured human fibroblasts to proliferate and produce tissue-like fibroplasia: a fibronectin matrix-dependent event, J. Cell. Physiol. 170 (1997) 69–80, https://doi.org/10.1002/(SICI)1097-4652(199701)170:1<69::AID-JCP8>3.0.CO;2-J.

[9] S. De Minicis, E. Seki, H. Uchinami, J. Kluwe, Y. Zhang, D.A. Brenner, R. F. Schwabe, Gene expression profiles during hepatic stellate cell activation in culture and in vivo, Gastroenterology 132 (2007) 1937–1946, https://doi.org/10.1053/j.gastro.2007.02.033.

[10] M. Sacchi, R. Bansal, J. Rouwkema, Bioengineered 3D models to recapitulate tissue fibrosis, Trends Biotechnol. 38 (2020) 623–636, https://doi.org/10.1016/j.tibtech.2019.12.010.

[11] M.J. Randall, A. Jüngel, M. Rimann, K. Wuertz-Kozak, Advances in the biofabrication of 3D skin in vitro: healthy and pathological models, Front. Bioeng. Biotechnol. 6 (2018) 154, https://doi.org/10.3389/fbioe.2018.00154.

[12] B. Hinz, G. Gabbiani, Cell-matrix and cell-cell contacts of myofibroblasts: role in connective tissue remodeling, Thromb. Haemost. 90 (2003) 993–1002, https://doi.org/10.1160/TH03-05-0328.

[13] P. Pakshir, B. Hinz, The big five in fibrosis: macrophages, myofibroblasts, matrix, mechanics, and miscommunication, Matrix Biol. J. Int. Soc. Matrix Biol. 68–69 (2018) 81–93, https://doi.org/10.1016/j.matbio.2018.01.019.

[14] F. Grinnell, Fibroblast biology in three-dimensional collagen matrices, Trends Cell Biol. 13 (2003) 264–269, https://doi.org/10.1016/s0962-8924(03)00057-6.

[15] J.L. Balestrini, S. Chaudhry, V. Sarrazy, A. Koehler, B. Hinz, The mechanical memory of lung myofibroblasts, Integr. Biol. Quant. Biosci. Nano Macro 4 (2012) 410–421, https://doi.org/10.1039/c2ib00149g.

[16] C.M. Artlett, Animal models of systemic sclerosis: their utility and limitations, Open Access Rheumatol. Res. Rev. 6 (2014) 65–81, https://doi.org/10.2147/OARRR.S50009.

[17] P. Marijic, L. Schwarzkopf, L. Schwettmann, T. Ruhnke, F. Trudzinski, M. Kreuter, Pirfenidone vs. nintedanib in patients with idiopathic pulmonary fibrosis: a retrospective cohort study, Respir. Res. 22 (2021) 268, https://doi.org/10.1186/s12931-021-01857-y.

[18] Ž.P. Kačarević, P.M. Rider, S. Alkildani, S. Retnasingh, R. Smeets, O. Jung, Z. Ivanišević, M. Barbeck, An introduction to 3D bioprinting: possibilities, challenges and future aspects, Materials 11 (2018) 2199, https://doi.org/10.3390/ma11112199.

[19] N. Sandbo, N. Dulin, Actin Cytoskeleton in Myofibroblast Differentiation: Ultrastructure Defining Form and Driving Function, Transl. Res. J. Lab. Clin. Med 158 (2011) 181–196, https://doi.org/10.1016/j.trsl.2011.05.004.

[20] A. Varadaraj, L.M. Jenkins, P. Singh, A. Chanda, J. Snider, N.Y. Lee, A.R. Amsalem-Zafran, M. Ehrlich, Y.I. Henis, K. Mythreye, TGF-β triggers rapid fibrillogenesis via a novel TβRII-dependent fibronectin-trafficking mechanism, Mol. Biol. Cell 28 (2017) 1195–1207, https://doi.org/10.1091/mbc.E16-08-0601.

[21] J.Y. Rao, R.E. Hurst, W.D. Bales, P.L. Jones, R.A. Bass, L.T. Archer, P.B. Bell, G. P. Hemstreet, Cellular F-actin levels as a marker for cellular transformation: relationship to cell division and differentiation, Cancer Res 50 (1990) 2215–2220.

[22] H. Suganuma, A. Sato, R. Tamura, K. Chida, Enhanced migration of fibroblasts derived from lungs with fibrotic lesions, Thorax 50 (1995) 984–989, https://doi.org/10.1136/thx.50.9.984.

[23] J.J. Tomasek, G. Gabbiani, B. Hinz, C. Chaponnier, R.A. Brown, Myofibroblasts and Mechano-Regulation of Connective Tissue Remodelling, Nat. Rev. Mol. Cell Biol. 3 (2002) 349–363, https://doi.org/10.1038/nrm809.

[24] A. Desmoulière, C. Chaponnier, G. Gabbiani, Tissue repair, contraction, and the myofibroblast, Wound Repair Regen. . Publ. Wound Heal. Soc. Eur. Tissue Repair Soc. 13 (2005) 7–12, https://doi.org/10.1111/j.1067-1927.2005.130102.x.

[25] T.E. King, M.I. Schwarz, K. Brown, J.A. Tooze, T.V. Colby, J.A. Waldron, A. Flint, W. Thurlbeck, R.M. Cherniack, Idiopathic pulmonary fibrosis: relationship between histopathologic features and mortality, Am. J. Respir. Crit. Care Med. 164 (2001) 1025–1032, https://doi.org/10.1164/ajrccm.164.6.2001056.

[26] X.-K. Zhao, L. Yu, M.-L. Cheng, P. Che, Y.-Y. Lu, Q. Zhang, M. Mu, H. Li, L.-L. Zhu, J.-J. Zhu, et al., Focal adhesion kinase regulates hepatic stellate cell activation and

liver fibrosis, Sci. Rep. 7 (2017) 4032, https://doi.org/10.1038/s41598-017-04317-0.
[27] Q. Xu, J.T. Norman, S. Shrivastav, J. Lucio-Cazana, J.B. Kopp, In Vitro models of TGF-beta-induced fibrosis suitable for high-throughput screening of antifibrotic agents, Am. J. Physiol. Ren. Physiol. 293 (2007) F631–F640, https://doi.org/10.1152/ajprenal.00379.2006.
[28] G. Serini, M.-L. Bochaton-Piallat, P. Ropraz, A. Geinoz, L. Borsi, L. Zardi, G. Gabbiani, The fibronectin domain ED-A is crucial for myofibroblastic phenotype induction by transforming growth factor-B1, J. Cell Biol. 142 (1998) 873–881.